ELSEVIER

Carbohydrate Research 297 (1997) 135–143

CARBOHYDRATE RESEARCH

Correlation between immunological activity, molar mass, and molecular structure of different (1 → 3)-β-D-glucans

Werner-Michael Kulicke *, Antje Iken Lettau, Heiko Thielking

Institut für Technische und Makromolekulare Chemie, Universität Hamburg, Bundesstraße 45, 20146 Hamburg, Germany

Received 14 June 1996; accepted 12 October 1996

Abstract

(1 → 3)-β-D-Glucans are said to be potential biomedical drugs against bacterial or viral infections and also show antitumour activity. These substances seem to enhance the activity of the immune system, but today there is no accepted mechanism, and not even any agreement on the parameters which influence the activity. Therefore, glucans with different structures and/or varying molar mass were characterized by multi-angle laser-light scattering coupled with size-exclusion chromatography in order to obtain the molar mass distribution and to gain an idea of the structure in solution. After ensuring that all samples were free of pyrogens, the Tumour-necrosis-factor-α release activity and the superoxide-anion released from human blood monocytes were measured in groups of samples with comparable polydispersity and degree of substitution. All glucans investigated, regardless of molar mass and solution structure, stimulate the investigated immunological measures more than a commercially available biomedical drug used for comparison. The greatest magnitude of molar mass was found to be about 550,000 g/mol for all the glucans investigated. Contrary to the cited literature, helical structures were not essential, and not even advantageous, for immunological activity. © 1997 Elsevier Science Ltd.

Keywords: Immunological activity; Glucan; Light-scattering; Size-exclusion chromatography

1. Introduction

Microbial polysaccharides of the type (1 → 3)-β-D-glucans, including schizophyllan, scleroglucan, and curdlan, belong to the group of so-called biological response modifiers, which have been attributed with antitumoural effects in many cases [1–6]. Furthermore, it is known from the literature that these effects cannot be traced back to a direct cytotoxic action, as is the case in chemotherapy. It would seem that an indirect antitumoural effect is present, i.e. one that is mediated by the immune system [7,8]. The principle upon which the immunomodulators operate is primarily based on the stimulation of certain non-specific and/or specific functions of the immune system. Hence, the use of this type of substance provides a possible alternative or adjuvant within existing thera-

* Corresponding author.

PII S0008-6215(96)00273-X

peutic programmes for the control of viral or bacterial infections or cancer. In contrast to other methods such as chemotherapy or vaccination, which are intended to damage the tumour directly, treatment with immunomodulators offers an opportunity of strengthening the body's natural defence system.

However, much controversy surrounds the biochemical and molecular principles of both the immunostimulation and the antitumoural activity. The same applies to the issue of whether these processes are interdependent and the conditions that are essential for this activity to occur in the biological response modifier substances. For instance, in connection with antitumoural effects, Yadomae et al. [9,10] and Kishida et al. [11] reported that high molar mass, a triple helix, and a β-(1 → 6)-branch are favourable structural parameters. In contrast to this, Saito et al. [12] and Gomaa et al. [13] described single helices as a requirement for this activity. Demleitner et al. [14] stated that it is exclusively the β-(1 → 3)-glycosidic linkage that is the essential structural feature for immunostimulatory and antitumoural effects, and no high molar mass is required.

The large number of results raised the question as to what influence the individual structural parameters really have on the effects mentioned above. Therefore it is the aim of this study to investigate the different influences of molar mass and solution structure (whether a coil-like or helical structure predominates) explicitly.

2. Experimental

Preparation of a homologous series of polymeric glucans.—The alkali-soluble glucans (0.1 M) were degraded by ultrasonic waves (Bronson Sonifier 450, temperature of the cooling liquid −15 °C, solution temperature ≤ 20 °C) to obtain a sample pool with different molar masses but without detaching the substituents, i.e. without destroying the chemical structure [15,16]. The molar mass obtained was controlled by sonification times ranging from 1 to 45 min (given as a number behind the sample name). The solutions were centrifuged at 600 rpm for 15 min, neutralised with H_2SO_4 (pH = 1), and dialysed against distilled water (cut off 10,000 Da). After separation of water-insoluble particles by filtration, the polymers were lyophilised and redissolved in a small volume of water. The final cleaning step was ion-exchange chromatography on DEAE Sephacel (Pharmacia, Uppsala, Sweden). Examinations were carried out to ensure that all samples were pyrogen-free. The degree of contamination by lipopolysaccharides was tested by the limulus-amolbocyte-lysate assay with the PYROGENT® gel plotting test kit (Byk Sangtec, Diezenbach, Germany).

^{13}C NMR spectroscopy.—The ^{13}C NMR investigations were carried out with an MSL-300 NMR spectrometer (Bruker, Karlsruhe, Germany), using approximately 8% (w/w) solutions in 0.1 M NaOD in 10-mm sample tubes; samples were internal referenced against methanol (δ 49).

Methylation analysis.—The procedure of Harris et al. [17] was used. Partially methylated alditol acetates were analysed by GC–MS on a capillary SE-52 column (50 m) using a VG Analytical 70-SE instrument with an ion-source as mass-selective detector. For quantitative analysis a Hewlett–Packard gas chromatograph 5890 was used (temperature program: 40 → 210 °C at 10 °C/min, then kept at 210 °C for 10 min).

Size-exclusion chromatography / multi-angle laser-light scattering.—Four TSK columns (Toso Haas, Stuttgart, Germany) with decreasing exclusion limit were coupled to a DAWN-F light scattering photometer (Wyatt Technology Corp., Santa Barbara, CA, USA) and from there the eluent was routed into a differential refractive index (DRI) detector Shodex RI SE 51 (Showa Denko, Tokyo, Japan) [18,19]. The carrier solution was deionized and double-distilled water containing 0.1 M $NaNO_3$ as polyelectrolyte and 0.02% (w/w) of NaN_3 as a bactericide. The solution was purified by filtration (0.1 μm) and degassed on-line (Knauer, Bad Homburg, Germany). The samples were dissolved in the carrier solution overnight without stirring. The injection volumes were 50 and 250 μL with an amount of 0.1 and 0.5 mg for each sample. The calibration of the photometer was done with ultra pure toluene and the normalisation of the fixed eighteen scattering angles was performed with a dispersed solution of gold of known diameter. The 'spider' plot method [20] was used for the determination of the interdetector volume. The signal of the DRI detector was routed to the photometer, which was interfaced to an AT computer.

Intrinsic viscosities.—The intrinsic viscosities were measured on a Zimm–Crothers low-shear rotary viscometer (Krannich, Göttingen, Germany).

Congo Red assay.—The wave length shift at maximum absorption of 0.88 μM Congo Red (Sigma) introduced by helical structures was recorded with a UV/visible spectrophotometer type PU 8700.

Cell isolation.—Human monocytes were obtained from 20 mL fresh blood. The samples were diluted in an equal volume of sterile saline, layered over 20 mL of lymphopreb (Nycomed, Oslo, Norway) in a 50 mL polypropylene conical tube and centrifuged for 30 min at 1800 rpm at 25 °C. The mononuclear cells were aspirated from the liquid/liquid interface (5 mL), added to 10 mL PBS-medium in a 15 mL conical polypropylene tube, and centrifuged for 10 min at 1200 rpm and 4 °C. The pellet was resuspended in 10 mL PBS, centrifuged again for 10 min at 4 °C and 1200 rpm, and then resuspended in 20 mL RMPI-1640 medium. The cell suspension was cultured in RMPI-1640 medium supplemented with 10% foetal calf serum, gentomycin, penicillin/streptomycin and with pyruvate at 37 °C in a 5% CO_2 atmosphere for 1 h. The monocytes were isolated with a cell scraper and diluted in 10 mL RMPI-1640 medium. A small volume (10 μL) was diluted 10-fold into trypan blue for the counting and viability estimation with a haemocytometer. The cell suspension was then diluted in RMPI-medium to achieve the desired final cell density.

Superoxide-anion production activity.—The measurement of the superoxide anions released from monocytes was based on the reduction of ferricytochrome *c* as assayed by the increase in its absorbency at 550 nm [21]. The monocytes were cultured in RMPI-1640 medium supplemented with 10% foetal calf serum, gentomycin, penicillin/streptomycin, and pyruvate at 37 °C in a 5% CO_2 atmosphere. Monocytes (1×10^5 cells/well, 96-well polystyrene microtiter plate) were activated by various glucans (20 μg/mL) for 2 h at 37 °C. After the addition of ferricytochrome *c* (6×10^{-5} M) to each well the absorbency values of individual wells were read at 550 nm with a microplate reader. In the test, a superoxide dismutase (100 μg/mL) was used as a blind well. Each value for optical density was calculated by subtracting the value of the control experiment without polysaccharide treatment. The nmols of O_2^- production were then calculated as described in the literature [21].

Tumour-necrosis-factor-α release activity.—The Tumour-necrosis-factor-α (TNF-α) release activity was measured by an immunoassay (Quantikine HS, R&D Systems, Inc., Minneapolis, USA). The monocytes were cultured in RMPI-medium supplemented with 10% foetal calf serum, gentomycin, penicillin/streptomycin and pyruvate at 37 °C in a 5% CO_2 atmosphere. The cells were activated with polysaccharides (20 μg/mL) for 24 h at 37 °C in 24-well-polystyrene microtiter plates. The supernatant cells were collected and centrifuged for 15 min at approximately 1000 rpm at room temperature. The assay procedure was carried out as described in the immunoassay information (for calculation see superoxide-anion production activity).

3. Results and discussion

Much controversy surrounds the issue of which structural conditions of glucans are essential for the antitumoural and immunological activity to occur in the biological response modifier substances [1,9–14]. In order to compare the influence of the molecular structure on the immunological activity, four different glucans were recovered from the fermentation processes of different fungi to obtain different structures. The native fermentation polysaccharides were obtained in cooperation with Professor F. Wagner and Dr. U. Rau (Institute of Biochemistry and Biotechnology, Technical University of Braunschweig) [22–24]. These glucans were then degraded ultrasonically to obtain samples with varying molar mass but with an unaltered structure. To describe the solution structure, the samples were first investigated by light-scattering, and after ensuring that all samples were free of pyrogens, the TNF-α release activity and the superoxide-anion release from human blood monocytes were measured. The results obtained are compared with the steric parameters and results obtained from a biomedical drug (BMD), based on schizophyllan, which is already in clinical use and commercially available in Japan [1].

Solution structure.—The chemical structure of the glucans was confirmed by ^{13}C NMR spectroscopy and methylation analysis [25–27]. The sample named **SR-glucan**, produced by *Sclerotium rolfsii*, is a (1 → 3)-β-D-glucan with β-(1 → 6)-linked glucose side-chains (one glucose unit) on about every third glucose unit along the backbone. The average degree of substitution was found to be DS = 0.31. The **SG-glucan** (DS = 0.33), produced by *Sclerotium glucanium*, the **MFN-glucan** (DS = 0.39), produced by *Monilinia fructigena*, and the **MFL-glucan** (DS = 0.38), produced by *Monilinia fructicola*, are also composed of a (1 → 3)-linked β-D-glucose backbone, with changing degrees of β-(1 → 6)-linked D-glucose branches (also one glucose unit).

In order to investigate the molecular dimensions, the native and the degraded samples were measured with light-scattering coupled to size-exclusion chro-

matography (SEC). The columns fractionate the samples by size and the multi-angle laser-light scattering photometer (MALLS) gives the molar mass and the root mean square radius for the eluent simultaneously, using Eq. (1) for diluted systems:

$$\frac{Kc}{R_\vartheta} = \frac{1}{M_w P(\vartheta)} \quad \text{with}$$

$$P(\vartheta) = 1 - a_1[2k\sin(\vartheta/2)]^2 + a_2[2k\sin(\vartheta/2)]^4 - \ldots \quad (1)$$

where K is a light scattering constant, containing the wavelength λ_0 of the incident light, the refractive index n_0 of the pure eluent and the refractive index increment dn/dc; c is the concentration, R_ϑ is the excess Rayleigh ratio and $P(\vartheta)$ a general form of a scattering function, from which a z-average root mean square radius $\langle R_G^2 \rangle_z^{0.5}$ can be derived. The molar mass distribution can be obtained by integration along the elution profile. As opposed to molar mass values calculated from normal size-exclusion chromatography, these results are not subject to the errors obtained when using a relative calibration curve for investigating samples which vary in their solution structure. Fig. 1 shows the elution profile (dotted lines) of an SEC measurement. In addition, the corresponding pair of molar mass and root mean square radius obtained from the on-line coupled MALLS is given for each point on the elution profile. Combining both pieces of information gives the corresponding distribution of molar mass and radius [18,19].

Fig. 2 shows the cumulative and differential forms for the molar mass distribution of the commercially available drug. The weight-average molar mass was found to be 550,000 g/mol, the number-average was found to be 390,000 g/mol. These results are close to the values given in the medical information of about 450,000 g/mol.

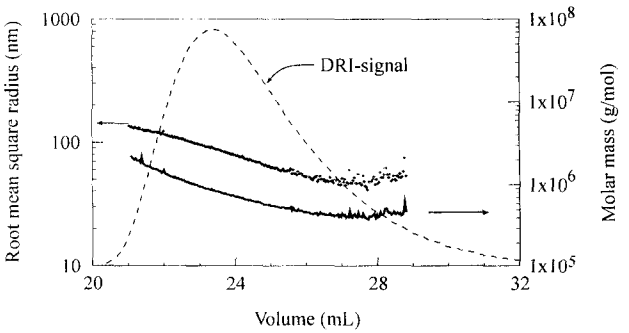

Fig. 1. Elution profile (differential refractive index-signal, dotted line), molar mass and corresponding root mean square radius of the MFL-10 sample measured by size-exclusion chromatography coupled on-line to multi-angle laser-light scattering (aq 0.1 M $NaNO_3$, 25 °C).

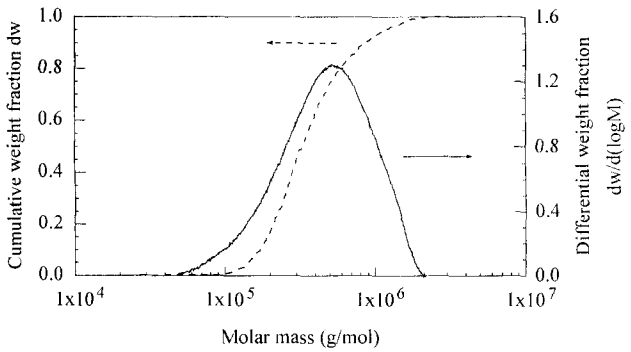

Fig. 2. Differential (logarithmic differentiation) and cumulative molar mass distribution of BMD, a schizophyllan-based medicine used in Japan for anti-cancer therapy. Determined in aq 0.1 M $NaNO_3$ by size-exclusion chromatography coupled on-line to multi-angle laser-light scattering, 25 °C.

To investigate the influence of molar mass on their immunological potential, the glucans were degraded ultrasonically. The use of this method ensures that the glucans obtained have varying molar masses but identical substitution structures [15,16]. The light scattering results (weight-average molar masses and root mean square radius) of the obtained sample pool are compiled in Table 1. The numbers after each sample name indicate the duration of ultrasonic degradation in minutes. The results for the native glucans (non-degraded) are slightly inaccurate because of the upper exclusion limit of the columns. The polydispersity values for all glucans were similar (about $M_w/M_n \approx 2$) but slightly higher than those measured for the biomedical drug.

If the radii of MFN-3 and SR-3 are compared with those of MFN-10 and SR-5 at corresponding values of molar mass, it can be seen that the latter are smaller. The dependence of the root mean square radius upon the molar mass correlates with the structure. For a rigid rod the molar mass is directly proportional to the root mean square radius (mass ~ length), for a hard sphere it is proportional to the cube of the geometrical radius (mass ~ radius^3). All other conformations can be found in-between these two borders. Conversely, if the root mean square radius and the molar mass are known, then the solution structure is also known. Schizophyllan is said to form a helical structure in aqueous solution, which can be treated mathematically like a rigid rod [28]. Japanese working groups postulate that the helical

Table 1
Molecular parameters of glucans, produced by *Sclerotium rolfsii* (*SR*), *Sclerotium glucanium* (*SG*), *Monilinia fructigena* (*MFN*), and *Monilinia fructicola* (*MFL*), determined in aq 0.1 M $NaNO_3$ by size-exclusion chromatography coupled on-line to multi-angle laser-light scattering and with a Zimm–Crothers viscosimeter

Sample [a]	M_w (g/mol)	$\langle R_G^2 \rangle_z^{0.5}$ (nm)	$[\eta]$ (mL/g)
Sclerotium rolfsii DS = 0.31			
SR-0	2,900,000	111	815
SR-1	1,200,000	91	510
SR-3	975,000	84	490
SR-5	550,000	58	330
SR-10	540,000	46	325
Sclerotium glucanium DS = 0.33			
SG-0	1,408,000	130	2126
SG-1	1,402,000	147	1900
SG-10	461,000	75	578
SG-45	280,000	43	337
Monilinia fructigena DS = 0.39			
MFN-0	1,570,000	143	1845
MFN-3	976,000	103	1035
MFN-5	876,000	96	1015
MFN-10	560,000	78	630
MFN-45	378,000	50	425
Monilinia fructicola DS = 0.38			
MFL-0	1,755,000	151	1326
MFL-1	1,665,000	144	1237
MFL-10	793,000	98	849
MFL-45	335,000	53	364

[a] The number behind the sample name indicates the duration of ultrasonic degradation in minutes.

structure is essential for antitumour activity [9,10]. As illustrated by the sample MFL-10 in Fig. 1, an on-line coupled MALLS photometer gives a corresponding pair of molar mass and root mean square radius for each point on the elution profile of the SEC columns. This information enables a 'form factor', ν, to be calculated for the solution structure. In Fig. 3 the root mean square radius values measured for the SR-5

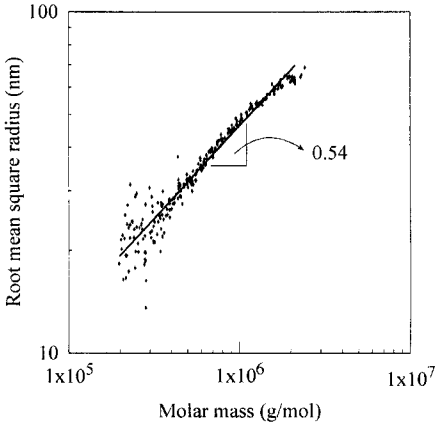

Fig. 3. Conformation plot – root mean square radius versus molar mass – of the SR-3 glucan. The slope of 0.54 given corresponds to a slightly expanded coil structure.

sample are plotted double-logarithmically against the molar mass values. The slope of $\nu = 0.54$ corresponds to the solution structure of a slightly expanded random coil, as known for example from linear dextran in water [29]. The mean values of ν for the four glucans are compiled in Table 2. The accuracy of the measured root mean square radius values depends on the size of the molecules. Using a HeNe-laser as light source and water as solvent gives values down to 20 nm accurately. The radius values of the low molecular mass tail of the small samples cannot be calculated (but the molar masses definitely can). The root mean square radius values of the small samples should therefore be lower than those given in Table 1. This inaccuracy has a slight influence on ν. In order to obtain a second value that would enable this inaccuracy to be estimated, an independent measure, the intrinsic viscosity, was correlated with the molar mass. This relationship, the well-known Mark–Houwink-equation, has an exponent of zero for spheres. For linear chain molecules forming a theta coil the Mark–Houwink exponent has a value

Table 2
Structural parameters of glucans, produced by *Sclerotium rolfsii, Sclerotium glucanium, Monilinia fructigena*, and *Monilinia fructicola* in aq 0.1 M $NaNO_3$. Calculations are based on the results from Table 1. The data for *Schizophyllum commune* are taken from Yanaki et al. [30]

Origin	Molar mass range (10^6 g/mol)	ν	$a_{calc.}$	a_η	k_η
Schizophyllum commune	0.1–0.5	–	–	1.2	–
	0.5–5.7	–	–	1.7	–
Sclerotium rolfsii, SR	0.5–2.9	0.54	0.63	0.61	0.1030
Sclerotium glucanium, SG	0.3–1.4	0.68	1.04	1.14	0.0002
Monilinia fructigena, MFN	0.4–1.6	0.70	1.10	1.02	0.0009
Monilinia fructicola, MFL	0.3–1.8	0.62	0.86	0.76	0.0260

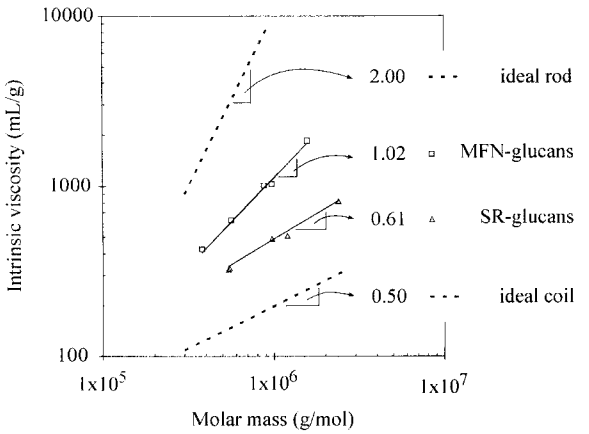

Fig. 4. Conformation plot – intrinsic viscosity versus molar mass. The dotted lines are the theoretic values calculated for ideal rods and coils. The measured data for the MFN- and the SR-glucans show the more coil-like or the more rod-like structure of the samples investigated.

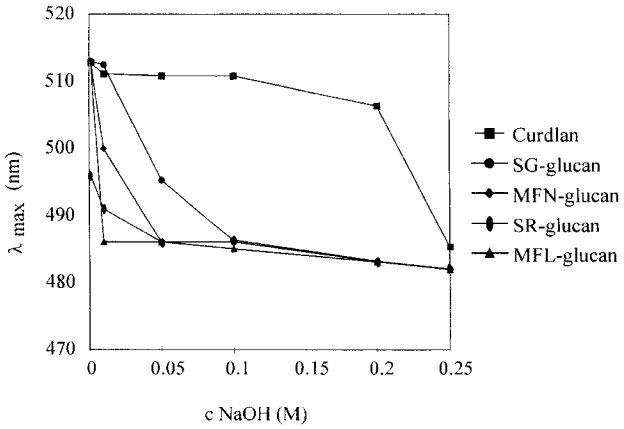

Fig. 5. Dependence of optical density of Congo Red/glucan complexes on the concentration of NaOH (1 mg glucan/0.88 μM Congo Red).

of 0.5. The better the solvent and the more rigid the molecular backbone, the more open the structure of the coil becomes, and the Mark–Houwink exponent increases up to a value of 2 for ideal rods. Because of its rod-like structure schizophyllan has an exponent of $a = 1.7$ [30]. The required intrinsic viscosities are given in Table 1, the calculated form factors are listed in Table 2. The plot in Fig. 4 of intrinsic viscosity versus molar mass for the MFN- and SR-glucans demonstrates the conformational change from ideal coil to ideal rod. In order to enable comparison of the values of the $\langle R_G^2 \rangle_z^{0.5} = k_\nu M_w^\nu$ and $[\eta] = k_a M_w^a$ relationships the ν values are transformed by the Flory theory into a_{calc} values [31]. The measured and the calculated values for the a-factor are equal within the limits of experimental error. The SG- and MFN-glucans have a rod-like structure, as does the BMD. The SR-glucan investigated, as mentioned above, has the solution structure of an expanded coil, and the MFL-glucan is to be found in-between. With $a = 0.76$ it is more like an expanded coil than a rod.

The rigidity which increases the a-values of the glucans beyond the values of expanded coils is expected to come from helical parts of the structure. The formation of complexes with Congo Red and the resulting shift of the maximum adsorption wavelength (λ_{max}-value) is a rapid method for detecting single helical structures. The aqueous solution of the MFN-glucan shows the greatest effect, which means it contains single helical structures. It shifts the λ_{max}-value from 477 to 513 nm. These single helices can be destroyed by adding sodium hydroxide. From the MFN-samples to the SG-glucan the shift in the λ_{max}-value decreases as expected, the SR-glucan does not show any wavelength shift (Fig. 5).

The present solution conformations of the glucans can be interpreted as random coil structures with differing portions of single helices (it can be imagined as shown in Fig. 6). For the immunological tests it might be acceptable to divide the glucans into two groups, rod-like and coil-like glucans.

Immunological activity.—To study the influence of molar mass and the effects of the solution structure on the immunological activity of the (1 → 3)-β-D-glucans, two laboratory tests were used: the TNF-α release and the production of superoxide radicals of monocytes treated with glucans.

The release of TNF-α by glucan-stimulated human blood monocytes represents an important anti-tumour mechanism [32]. At first the monocytes were stimulated with different concentrations of BMD to obtain

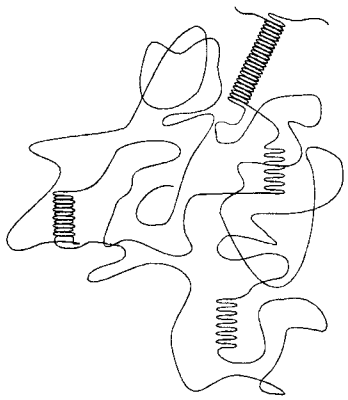

Fig. 6. Modulation of a random coil structure with partially helical areas, which are responsible for the rigidity of the molecules and the complexation of Congo Red.

Table 3
TNF-α release by human blood monocytes cultured with various concentrations of BMD and native glucan (ΔTNF-α = TNF-α_{glucan} − TNF-$\alpha_{control}$)

Glucan	ΔTNF-α release (pg/50,000 cells) [a]					
	Concentration of polysaccharide (μg/mL)					
	20	50	200	500	1000	10,000
BMD	70 ± 1.3	60 ± 2.7	61 ± 2.3	60 ± 1.0	64 ± 1.6	40 ± 3.6
MFN-0	84 ± 12	82 ± 17	80 ± 16	76 ± 17	69 ± 15	52 ± 2.6
SR-0	128 ± 16	117 ± 12	116 ± 10	110 ± 14	98 ± 7.0	49 ± 1.8

[a] The errors indicated are the standard deviations of the twelve experiments conducted with three different blood samples.

the optimal test concentration. The BMD concentration ranging from 20 to 1000 μg/mL was found to effect the TNF-α release relative constantly (Table 3). This experiment was repeated with the native glucans MFN-0 and SR-0 and the influence of concentration was again not significant. The other results were therefore obtained by monocytes treated with a small amount of glucans.

When treating the human blood monocytes with the samples obtained (using a constant concentration, nearly constant polydispersity, nearly constant degree of substitution, but different molar mass and different solution structure) the most surprising result was that all the glucans were more potent stimulators for TNF-α production than the BMD applied.

The numerical results are summarised in Table 4. Glucans with low molar mass increase the TNF-α release more than high-molar-mass samples. In Fig. 7 the TNF-α release is plotted against the molar mass for the MFN- and SR-glucans. The maximum values are located around 550,000 g/mol, which is also the molar mass range of the BMD. Fig. 7 also demonstrates the influence of ordered structures. At the maximum of TNF-α production, samples SR-5, MFN-10 and BMD have comparable molar mass values but different solution structures. The SR-glucan with the random coil structure gives much better results than the partially ordered MFN or the BMD. The increasing presence of helical conformation diminishes the TNF-α release. These results contradict the statement that ordered structures are necessary to release a great quantity of the cytokine, as described in the literature [9–11].

Incomplete reduced forms of oxygen, including superoxide, can play a major role in anti-microbial, anti-tumour, and inflammatory functions of monocytes too. The primary reaction is the one-electron reduction of oxygen to O_2^- through the action of a cyanide-resistant NADPH oxidase. The results of experiments with glucan-treated monocytes show a dependence of 'oxidative' or 'respiratory' burst upon the molar mass of polysaccharides. In Table 4 the overall O_2^- values are listed for all glucans. The interpretation is similar to that for TNF-α release. All glucans, except the polysaccharides from *Sclerotium glucanium*, show the same tendency. The lower molar mass samples stimulate superoxide production

Table 4
Superoxide-anion production and TNF-α release by human blood monocytes cultured with glucan samples, varying in molar mass (concentration of the glucans, 20 μg/mL; ΔTNF-α = TNF-α_{glucan} − TNF-$\alpha_{control}$, ΔO_2^- = $O_{2\,glucan}^- - O_{2\,control}^-$)

Sample	ΔTNF-α release [a] (pg/5 × 10^4 cells)	ΔO_2^- production [b] (nmol/10^5 cells)
Sclerotium rolfsii		
SR-0	128 ± 16	1.9 ± 0.15
SR-1	132 ± 10	2.7 ± 0.11
SR-3	129 ± 20	3.2 ± 0.14
SR-5	283 ± 30	4.1 ± 0.10
SR-10	259 ± 25	4.1 ± 0.05
Sclerotium glucanium		
SG-0	108 ± 4	3.0 ± 0.30
SG-1	117 ± 5	3.2 ± 0.20
SG-10	201 ± 17	3.1 ± 0.12
SG-45	194 ± 13	3.1 ± 0.05
Monilinia fructigena		
MFN-0	84 ± 12	1.2 ± 0.18
MFN-3	90 ± 12	1.6 ± 0.20
MFN-5	119 ± 14	1.6 ± 0.05
MFN-10	215 ± 17	3.3 ± 0.14
MFN-45	187 ± 16	3.6 ± 0.22
Monilinia fructicola		
MFL-0	100 ± 6	2.6 ± 0.19
MFL-1	122 ± 14	2.8 ± 0.11
MFL-10	251 ± 19	3.5 ± 0.30
MFL-45	196 ± 5	3.2 ± 0.14

[a] The errors indicated are the standard deviations of 12 experiments conducted with three different blood samples.
[b] The errors indicated are the standard deviations of 32 experiments conducted with four different blood samples.

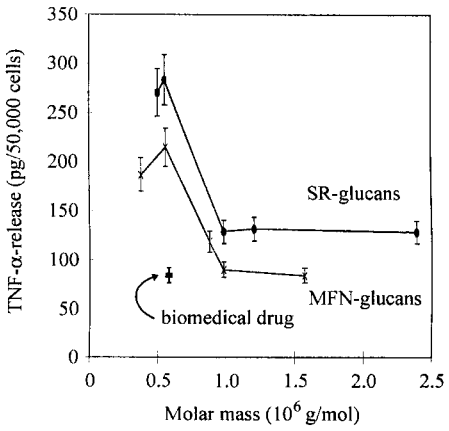

Fig. 7. Relationship between molar mass and TNF-α release for glucans with differing solution structures.

more than those with a high molar mass do. The superoxide release from monocytes treated with the SG-glucans seems to be independent of molar mass. The coil-like SR-glucan seems to be the most potent activator and the rod-like BMD the lowest activator of superoxide production.

Characterization of the molar mass and the solution structure of β-(1 → 3)-D-glucose polymers with β-(1 → 6)-linked glucose side-chains and the correlation of the results with immunological data leads to the following conclusions:

- All glucans investigated, irrespective of their molar mass and solution structure, stimulate the release of TNF-α and the superoxide more than the biomedical drug BMD;
- The magnitude of the molar mass used in BMD (550,000 g/mol) was the most potent molar mass range for all the glucans investigated;
- Contrary to some cited literature [1,9,10], helically ordered structures are not essential or even advantageous for immunological activity.

To gain greater insight into this important topic, it would be useful to investigate glucans with more defined structures and modified substituents. Furthermore, we would like to test these glucans to stimulate other immunological parameters in vitro and in vivo. Confirmation of these results with the other immunological tests would also be of great interest.

4. Glossary

a	exponent of Mark–Houwink ($[\eta]$M) equation
a_1, a_2, ...	virial coefficients
c	concentration
DRI	differential refractive index
dn/dc	refractive index increment
K	light scattering constant, equal to $4\pi^2(dn/dc)^2 n_0^2/N_A\lambda_0^4$
k_η	constant in $[\eta]$–M-relationship
k	$2\pi n_0/\lambda_0$
M	molar mass
$M_{n/w/z}$	number/weight/z-average molar mass
MALLS	multi-angle laser-light scattering
n_0	refractive index of pure solvent
N_A	Avogadro number
$P(\vartheta)$	scattering function
$\langle R_G^2 \rangle^{0.5}$	root mean square radius
$\langle R_G^2 \rangle_z^{0.5}$	z-average root mean square radius
R_ϑ	excess Rayleigh ratio

Greek Characters

ϑ	scattering angle
$[\eta]$	intrinsic viscosity
ν	exponent of RM equation
λ_0	vacuum wavelength of incident light

Acknowledgements

This work was kindly supported by the Deutsche Forschungsgemeinschaft (DFG). The authors would like to thank Professor Thiele and Dr. Schreiber (University Hospital of Hamburg) for their encouragement and discussions on immunological research. Special thanks go to Professor F. Wagner and Dr. Rau (University Braunschweig) for supplying the native fermentation polysaccharides.

References

[1] H. Furue, *Drugs Today*, 23 (1987) 335–346.
[2] M. Bruneteau, J. Fabre, J. Perret, G. Michel, P. Ricci, J.P. Joseleau, J. Kraus, M. Schneider, W. Blaschek, and G. Franz, *Carbohydr. Res.*, 175 (1988) 137–143.
[3] P.P. Singh, R.L. Whistler, R. Tokuzen, and W. Nakahea, *Carbohydr. Res.*, 37 (1974) 245–247.
[4] N.R. Diluzio, D.L. Williams, R.B. McNamee, B.F. Edwards, and A. Kitahama, *Int. J. Cancer*, 24 (1979) 773–779.
[5] T. Kiho, M. Katsuragawa, K. Nagai, and S. Ukai, *Carbohydr. Res.*, 224 (1992) 237–243.
[6] R.G. Ovodova, V.E. Glazkova, L.V. Mikheyskaya, V.J. Molchanova, V.V. Isakov, Y.S. Ovodov, and L.E. Fernandez-Molina, *Carbohydr. Res.*, 223 (1992) 221–226.
[7] J.K. Czop and J. Kay, *J. Exp. Med.*, 173 (1991) 1511–1520.

[8] G. Chihara, *J. Immunol. Immunopharmacol.*, IV (1983) 85–96.
[9] N. Ohno, N. Asada, Y. Adachi, and T. Yadomae, *Biol. Pharm. Bull.*, 18 (1995) 126–133.
[10] N. Ohno, N. Noriko, N. Miura, N. Chiba, Y. Adachi, and T. Yadomae, *Biol. Pharm. Bull.*, 18 (1995) 1242–1247.
[11] E. Kishida, Y. Sone, and A. Misaki, *Carbohydr. Polymers*, 17 (1992) 89–95.
[12] H. Saito, Y. Yoshioka, N. Uehara, J. Aketagawa, S. Tanaka, and Y. Shibata, *Carbohydr. Res.*, 217 (1991) 181–190.
[13] K. Gomaa, J. Kraus, G. Franz, and H. Röper, *Carbohydr. Res.*, 217 (1991) 153–161.
[14] S. Demleitner, J. Kraus, and G. Franz, *Carbohydr. Res.*, 226 (1992) 239–246.
[15] K. Tababata, W. Ito, T. Kojima, S. Kawabata, and A. Misaki, *Carbohydr. Res.*, 89 (1981) 121–135.
[16] W.-M. Kulicke, M. Otto, and A. Baar, *Makromol. Chem.*, 194 (1993) 751–765.
[17] P.J. Harris, R.J. Henry, A.B. Blakeny, and B.A. Stone, *Carbohydr. Res.*, 127 (1984) 59–73.
[18] W.-M. Kulicke and N. Böse, *Coll. Polym. Sci.*, 262 (1984) 197–207.
[19] W.-M. Kulicke, D. Roessner, and W. Kull, *Starch / Stärke*, 45 (1993) 445–450.
[20] P.J. Wyatt, *Anal. Chim. Acta*, 272 (1993) 1–40.
[21] H. Pick and D. Mizel, *J. Immunol. Methods*, 46 (1981) 211–226.
[22] U. Rau, E. Gura, E. Olszewski, and F. Wagner, *J. Industial Microbiol.*, 9 (1992) 19–26, and references therein.
[23] F. Pilz, G. Auling, D. Stephan, U. Rau, and F. Wagner, *Exp. Mycology*, 15 (1991) 181–192, and references therein.
[24] W.-M. Kulicke and J. Lehmann, *Chem.-Ing. Tech.*, 12 (1986) 967–969.
[25] F. Santamaria, F. Reyes, and R. Lahoz, *J. Gen. Microbiol.*, 109 (1978) 2878–2893.
[26] K.W. Buck, A.W. Chen, A.G. Dickerson, and E. Chain, *J. Gen. Microbiol.*, 51 (1973) 337–352.
[27] T.B. Stokke, A. Elgsaeter, C. Hara, S. Kitamura, and K. Takeor, *Biopolymers*, 33 (1993) 561–573, and references therein.
[28] R. Oertel and W.-M. Kulicke, *Rheologica Acta*, 30 (1991) 140–150.
[29] J. Brandrup and E.H. Immergut (Eds.), in *Polymer Handbook*, Wiley, New York, 1975.
[30] T. Yanaki, T. Norisuye, and H. Fujita, *Macromolecules*, 13 (1980) 1462–1466.
[31] T.G. Fox, J.C. Fox, and P.J. Flory, *J. Am. Chem. Soc.*, 73 (1951) 1901.
[32] I.M. Roitt, J. Brostoff, and D.K. Male, *Kurzes Lehrbuch der Immunologie*, Thieme, Stuttgart, 1991.